Supplement of Atmos. Meas. Tech., 18, 2509–2521, 2025
https://doi.org/10.5194/amt-18-2509-2025-supplement

Atmospheric Measurement Techniques
Open Access
EGU

Supplement of

A comprehensive characterization of empirical parameterizations for OH exposure in the Aerodyne Potential Aerosol Mass Oxidation Flow Reactor (PAM-OFR)

Qianying Liu et al.

Correspondence to: Dan Dan Huang (huangdd@saes.sh.cn) and Yong Jie Li (yongjieli@um.edu.mo)

List of the supporting information:

Tables.

Figures.

Tables.

Table S1: List of 25 sets of OFR185 trace-gas decay experiments under different conditions. SO_2 or CO was used as the source of external OH reactivity (OHR_{ext}). Each set of experiments was performed under 5–9 lamp intensity settings.

Experiment ID	Species	Initial concentration(ppb)	OHR_{ext} (s^{-1})	Residence time (s)	Water vapor mixing ratio (%)
1	SO_2	182.8	4.27	33.3	0.58
2		191.0	4.46	33.3	0.63
3		193.2	4.52	33.3	0.64
4		274.0	6.40	99.8	0.79
5		291.0	6.80	99.8	0.69
6		331.0	7.74	295.6	1.60
7		366.0	8.55	181.4	1.55
8		379.4	8.87	33.3	0.63
9		380.3	8.89	33.3	1.05
10		383.1	8.96	33.3	0.87
11		489.4	11.44	61.4	0.62
12		513.0	11.99	199.5	0.66
13		650.0	15.19	181.4	2.72
14		750.0	17.53	181.4	1.98
15		789.1	18.45	33.3	0.74
16		973.2	22.75	33.3	1.19
17		8556.4	197.98	61.4	0.52
18		8556.4	200.00	33.3	0.38
19		8718.6	203.79	33.3	0.53
20	CO	10247.8	60.58	33.3	1.15
21		12298.2	72.70	33.3	0.86
22		103238.4	610.27	33.3	0.95
23		103852.8	613.91	33.3	0.86
24		207445.7	1226.27	33.3	0.97
25		207496.6	1226.58	33.3	0.89

Table S2: List of 37 sets of OFR254 trace-gas decay experiments under different conditions. SO_2 or CO was used as the source of OHR_{ext}. Each set of experiments was performed under 5–9 lamp intensity settings.

Experiment ID	Species	Initial concentration (ppb)	OHR_{ext} (s^{-1})	Input O_3 concentration (ppm)	Residence time (s)	Water vapor mixing ratio (%)	Relative humidity (%)
1	SO_2	286.2	6.69	4.27	69.6	1.65	27.8
2		283.3	6.62	5.91	69.0	2.46	39.6
3		283.8	6.63	6.17	69.0	0.99	18.1
4		289.9	6.78	6.30	69.0	1.52	28.7
5		575.5	13.45	6.20	69.0	1.07	17.0
6		575.2	13.44	6.08	69.0	2.45	43.8
7		583.5	13.64	6.15	69.0	1.62	29.2
8		868.6	20.30	6.23	69.0	2.22	44.0
9		874.7	20.45	6.05	69.0	1.57	27.7
10		868.9	20.31	6.32	69.0	0.97	16.9
11		454.9	10.63	7.77	69.0	0.96	17.1
12		450.2	10.52	8.16	69.0	2.17	41.8
13		450.7	10.53	6.58	69.0	1.41	28.6
14		737.9	17.25	8.32	69.0	0.88	16.9
15		746.8	17.46	7.77	69.0	2.20	39.9
16		747.0	17.46	9.38	69.0	1.50	26.8
17		204.0	4.77	2.62	34.4	2.11	42.8
18		201.9	4.72	3.00	34.4	1.32	27.9
19		196.9	4.60	2.90	34.4	0.94	19.0
20		282.6	6.61	6.07	34.4	0.79	17.3
21		572.9	13.39	6.11	34.4	0.82	17.6
22		908.6	21.24	6.08	34.4	0.78	17.3
23		204.7	4.78	4.47	43.7	0.86	18.2
24		402.8	9.41	5.47	47.4	2.14	42.0
25		459.9	10.75	5.34	54.0	1.91	36.4
26		840.2	19.64	9.82	111.5	1.74	36.1
27		262.7	6.14	8.23	70.9	2.27	43.0
28		430.8	10.07	8.19	70.6	2.23	45.5
29		260.1	6.08	13.17	69.6	2.38	40.6
30		511.4	11.95	19.39	125.5	2.61	45.2

Experiment ID	Species	Initial concentration (ppb)	OHR_{ext} (s^{-1})	Input O_3 concentration (ppm)	Residence time (s)	Water vapor mixing ratio (%)	Relative humidity (%)
31		4909.4	29.02	3.15	19.8	0.91	19.0
32		4685.6	27.70	5.06	37.4	0.83	20.8
33		4958.3	29.31	4.13	47.1	0.78	15.9
34	CO	4829.8	28.55	5.59	69.4	2.20	43.3
35		4358.0	25.76	2.95	34.5	1.78	36.2
36		5034.5	29.76	4.82	46.8	2.18	39.4
37		4438.5	26.24	12.95	95.2	2.25	40.4

Table S3: In OFR185 mode, the range of various experimental conditions involved in the different datasets when fitting parameters *a*–*f* and evaluating their applicability.

Figure #	Residence time (s)	Water vapor mixing ratio (%)	Output O_3 concentration (molecules cm^{-3})	External OHR (s^{-1})	OHR source
Fig. 1a1	33	0.54–1.48	1.44×10^{12}–1.89×10^{14}	4–23	SO_2
Fig. 1a2	33–200				
Fig. 1a3					
Fig. 1b1	33–200	0.49–0.99	1.44×10^{12}–2.03×10^{15}	4–18	SO_2
Fig. 1b2		0.49–2.76			
Fig. 1b3					
Fig. 1c1	33–296	0.49–1.62	1.44×10^{12}–6.79×10^{13}	4–23	SO_2
Fig. 1c2			1.44×10^{12}–2.03×10^{15}		
Fig. 1c3					
Fig. 2a	33–296	0.49–2.76	1.44×10^{12}–2.03×10^{15}	4–23	SO_2
Fig. 2b				4–204	
Fig. 2c					
Fig. 3a	33–296	0.38–2.76	1.44×10^{12}–2.03×10^{15}	4–204	SO_2
Fig. 3b	33	0.85–1.17	1.95×10^{12}–1.88×10^{14}	61–1227	CO
Fig. 3c	33–296	0.38–2.76	1.44×10^{12}–2.03×10^{15}	4–1227	SO_2 + CO
Fig. S3a1	100–296	0.63–2.76	8.16×10^{12}–2.03×10^{15}	6–18	SO_2
Fig. S3a2	33–296				
Fig. S3a3					
Fig. S3b1	33–296	1.04–2.76	3.31×10^{12}–1.16×10^{15}	8–23	SO_2
Fig. S3b2		0.49–2.76			
Fig. S3b3					
Fig. S3c1	33–296	0.50–2.76	8.45×10^{13}–2.03×10^{15}	4–23	SO_2
Fig. S3c2			1.44×10^{12}–2.03×10^{15}		
Fig. S3c3					

Table S4: In OFR254 mode, the range of various experimental conditions involved in the different datasets when fitting parameters *x*–*z* and evaluating their applicability.

Figure #	External OHR (s^{-1})	Output O_3 concentration (molecules cm^{-3})	r_{O3}	OHR source
Fig. 4a1	5–14	6.46×10^{13}–4.77×10^{14}	0.42–1.00	SO_2
Fig. 4a2	5–21			
Fig. 4a3				
Fig. 4b1	5–21	6.46×10^{13}–1.62×10^{14}	0.66–1.00	SO_2
Fig. 4b2		6.46×10^{13}–4.77×10^{14}		
Fig. 4b3				
Fig. 4c1	6–20	1.05×10^{13}–3.24×10^{14}	0.69–0.90	SO_2
Fig. 4c2			0.61–0.99	
Fig. 4c3				
Fig. 5a	5–21	6.46×10^{13}–4.77×10^{14}	0.42–1.00	SO_2
Fig. 5b	26–30	7.28×10^{13}–3.19×10^{14}	0.66–1.00	CO
Fig. 5c	5–30	6.46×10^{13}–4.77×10^{14}	0.42–1.00	SO_2 + CO

Table S5: In OFR185 mode, the parameters *a*–*f* for the $OH_{exp,\ est}$ estimation were obtained from different data sets.

OFR185	Figure #	Data sets	FP	Coefficient					
				a	b	c	d	e	f
Residence time	Fig. 1a1	short t	$FP_{st,\ 185}$	4.2566	0.57973	-0.062233	0.47836	0.0027988	0.55255
	Fig. 1a2	adding long t							
	Fig. 1a3		$FP_{et,\ 185}$	4.5772	0.58603	-0.10617	0.40819	0.004321	0.50352
Water vapor mixing ratio	Fig. 1b1	low H_2O	$FP_{lH2O,\ 185}$	5.5822	0.62134	-0.23848	0.27915	0.0071196	0.42689
	Fig. 1b2	adding high H_2O							
	Fig. 1b3		$FP_{eH2O,\ 185}$	4.2899	0.70966	-0.21378	0.23242	0.0052289	0.39371
Output O_3 concentration	Fig. 1c1	low $O_{3,\ out}$	$FP_{lO3,\ 185}$	3.3154	2.3046	-1.74	0.033076	0.0061601	0.29402
	Fig. 1c2	adding high $O_{3,\ out}$							
	Fig. 1c3		$FP_{eO3,\ 185}$	3.5229	2.2995	-1.7422	0.027553	0.0050063	0.29182
External OHR	Fig. 2a	low OHR_{ext}	$FP_{lOHR,\ 185}$	3.2404	0.74398	-0.13922	0.26786	0.0026332	0.4917
	Fig. 2b	adding high OHR_{ext}							
	Fig. 2c		$FP_{eOHR,\ 185}$	3.5103	0.62481	-0.079114	0.36805	0.0041654	0.38722
OHR source	Fig. 3a	SO_2	$FP_{SO2,\ 185}$	3.2759	0.65745	-0.10638	0.23087	0.0050212	0.24198
	Fig. 3b	CO	$FP_{CO,\ 185}$	4.1575	0.55935	-0.86966	-0.17843	0.089848	-0.2993
	Fig. 3c	SO_2 + CO	$FP_{SO2\&CO,\ 185}$	2.1665	0.78424	-0.13214	0.089098	0.0036945	0.03358

Table S6: In OFR254 mode, the parameters *x*–*z* of the $OH_{exp,\ est}$ estimation were obtained from different data sets.

OFR254	Figure #	Data sets	FP	Coefficient		
				x	y	z
External OHR	Fig. 4a1	low OHR_{ext}	$FP_{lOHR,\ 254}$	12.798	0.34588	0.085063
	Fig. 4a2	adding high OHR_{ext}				
	Fig. 4a3		$FP_{eOHR,\ 254}$	13.151	-17.172	0.12986
Input O_3 concentration	Fig. 4b1	low $O_{3,\ in}$	$FP_{lO3,\ 254}$	13.459	-19.285	0.11153
	Fig. 4b2	adding high $O_{3,\ in}$				
	Fig. 4b3		$FP_{eO3,\ 254}$	13.325	-19.393	0.12029
r_{O3}	Fig. 4c1	medium r_{O3}	$FP_{mrO3,\ 254}$	12.989	-9.9122	0.13684
	Fig. 4c2	adding extended r_{O3}				
	Fig. 4c3		$FP_{erO3,\ 254}$	13.213	-18.921	0.13111
OHR source	Fig. 5a	SO_2	$FP_{SO2,\ 254}$	13.145	-18.669	0.13316
	Fig. 5b	CO	$FP_{CO,\ 254}$	16.161	-92.945	0.11466
	Fig. 5c	SO_2 + CO	$FP_{SO2\&CO,\ 254}$	13.075	-15.698	0.13741

Figures.

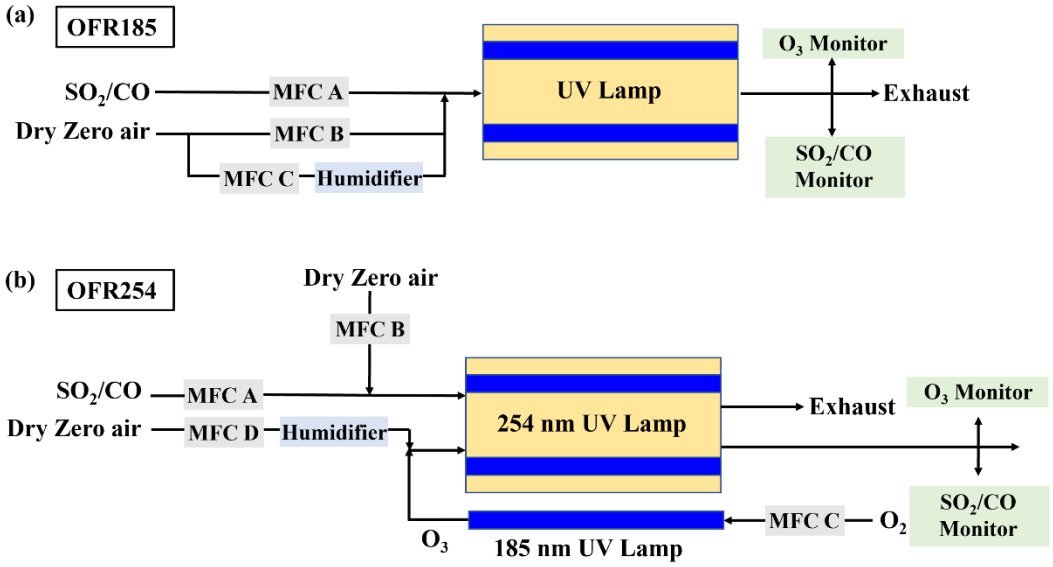

Figure S1: The schematics of the PAM-OFR experimental setup for trace-gas decay experiments in (a) OFR185 mode and (b) OFR254 mode.

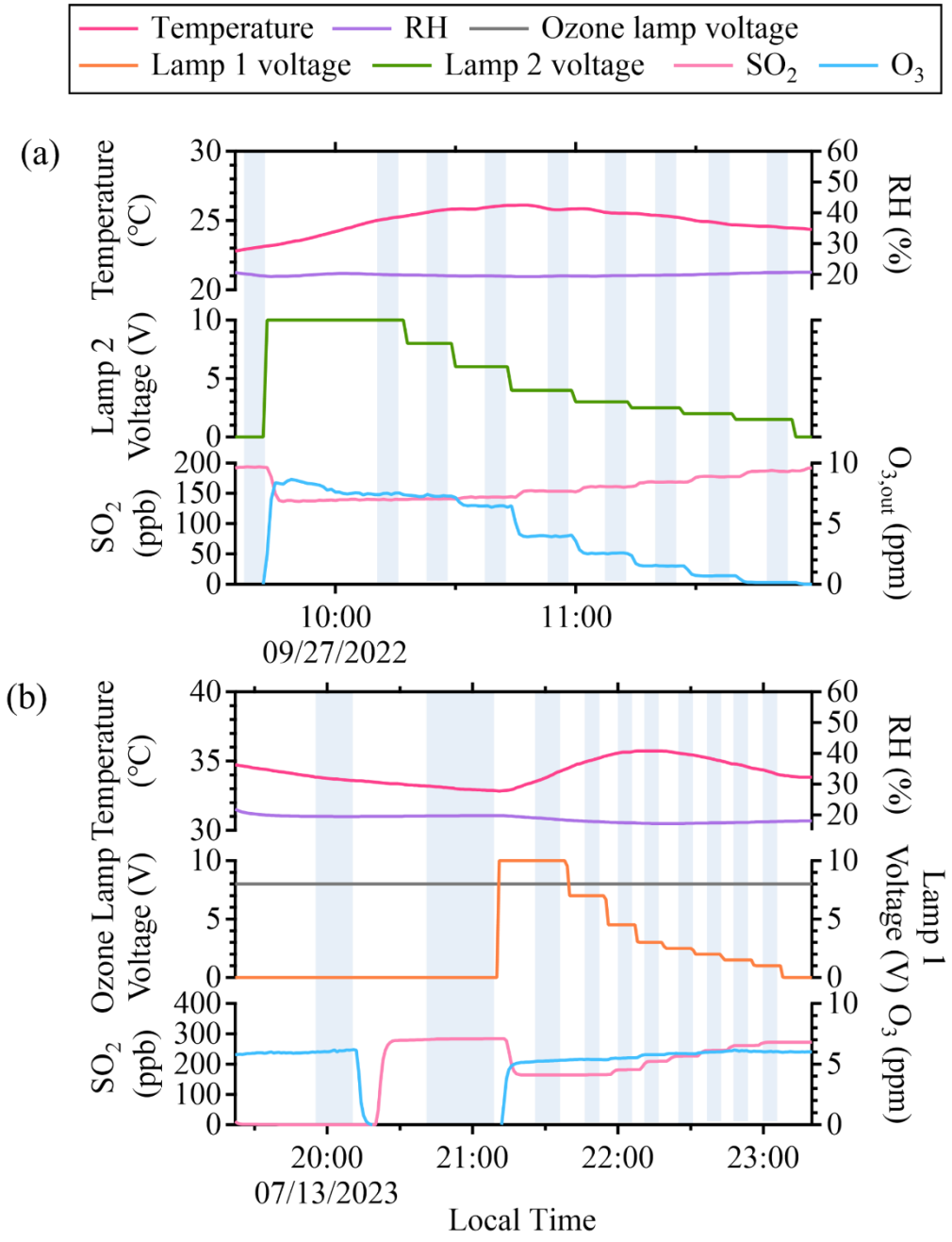

Figure S2: The examples of a set of experiments conducted in (a) the OFR185 mode and (b) the OFR254 mode, respectively. A set of experiments was operated with light voltage settings stepping decreasing from 10V to 0V. The highlighted areas indicate the periods when all conditions had reached a steady state and the tracer gas was sampled.

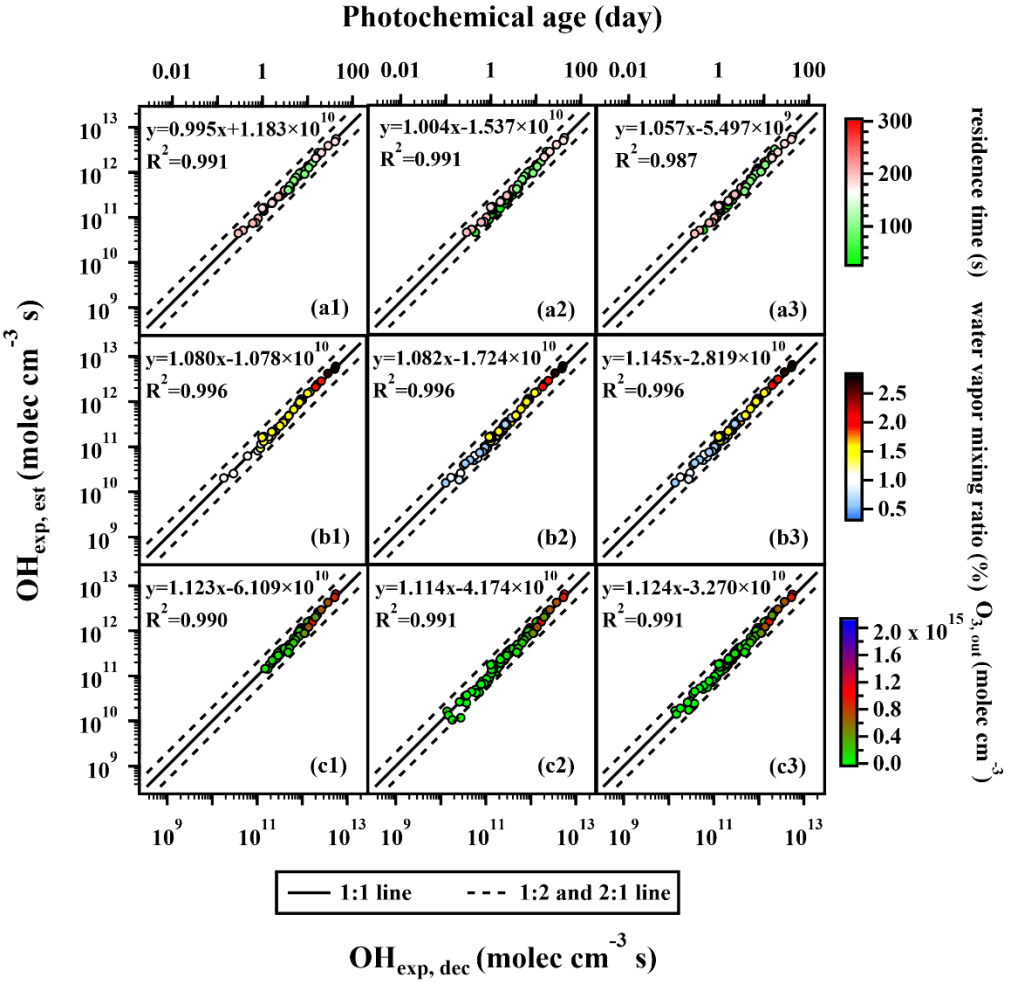

Figure S3: The regression results of $OH_{exp,\ est}$ and $OH_{exp,\ dec}$ when variations occurred in (a1–a3) residence time, (b1–b3) water vapor mixing ratio, and (c1–c3) output O_3 concentration under atmospheric relevant OHR_{ext} level (4–23 s^{-1}). Compared to panels a1, b1, and c1, panels a2, b2, and c2 respectively incorporated additional data points with lower t, H_2O, and $O_{3,\ out}$ values, but still utilized the fitting parameters *a*–*f* obtained from the higher condition range to estimate $OH_{exp,\ est}$. In panels a3, b3, and c3, all data points within the extended condition range were used to re-fit the parameters *a*–*f*, which were employed to estimate $OH_{exp,\ est}$.

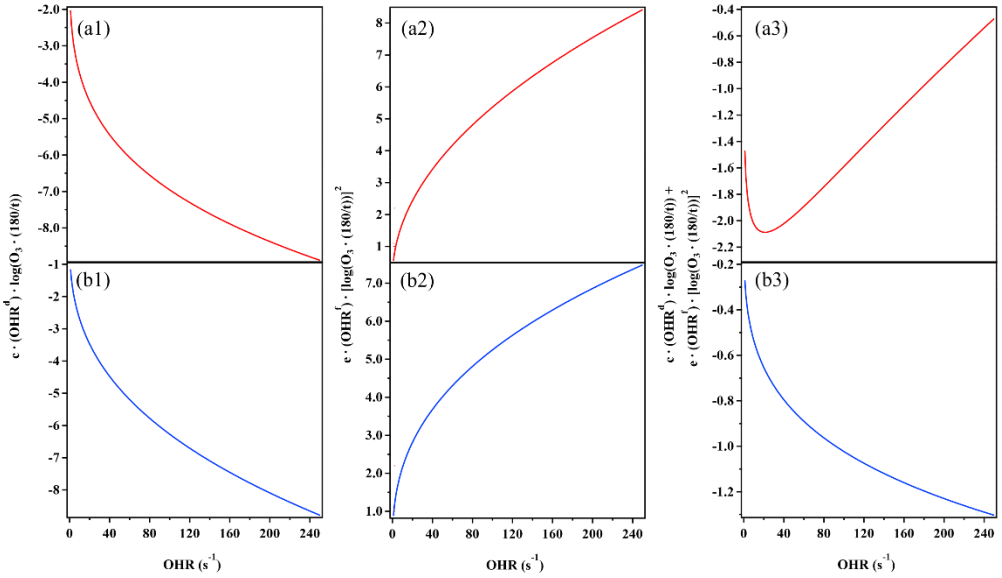

Figure S4: (a1–a3) The variations of $c \times OHR_{ext}^{d} \times \log(O_{3,\,out} \times 180/t)$, $e \times OHR_{ext}^{f} \times [\log(O_{3,\,out} \times 180/t)]^2$ and their sum with respect to OHR_{ext} when using the fitted values of *c*–*f* (-0.13922, 0.26786, 0.0026332, 0.4917) obtained from the low OHR_{ext} data points. (b1–b3) The variations of $c \times OHR_{ext}^{d} \times \log(O_{3,\,out} \times 180/t)$, $e \times OHR_{ext}^{f} \times [\log(O_{3,\,out} \times 180/t)]^2$ and their sum with respect to OHR_{ext} when using the fitted values of *c*–*f* (-0.079114, 0.36805, 0.0041654, 0.38722) obtained from the data points with a wider range of OHR_{ext} condition.